SINGLE IMAGE DEHAZING VIA TV-ℓ_1 MINIMIZATION

Anonymous ICME submission

ABSTRACT

In this paper, we propose a novel algorithm to remove haze from single image based on total variation minimization. This algorithm is based on two observations. One is that clear-day images have more contrast than images plagued by bad weather; the other is that the variations of *atmospheric veil*, which mainly depends on the distance of objects to the viewer, tend to be smooth. Therefore, the color and visibility can be recovered by maximizing the the atmospheric veil assuming it is smooth most of the time, which is equivalently maximizing the contrast of the hazy images. The total variation minimization is adapted here to maximize the atmospheric veil while preserving the discontinuities. The results shows that our algorithm can handle most of the hazy images. To demonstrate the effectiveness of our algorithm, we evaluate it using both true scene images and synthetic ones. A comparative study and quantitative evaluation is proposed with a few other state of the art algorithms which demonstrates that similar or better quality results are obtained.

Index Terms— Image dehazing, Visibility restoration, Total variation minimization

1. INTRODUCTION

The photographs we get in our daily life are easily plagued by the aerosols suspended in the medium, such as dust, mist, or fumes. The rays reflected by the objects surfaces are not only attenuated by the existing aerosols but also blended with the airlight when they reach the observers. Therefore, the quality of photographs taken in the hazy scenes are seriously degraded. They appear poor visibility and contrast lost of the scene.

The goal of dehazing algorithms is to recover color and details of scene from hazy images. There are many circumstances that accurate dehazing algorithms are needed. In computer vision, most existing applications assume that the radiance from a scene point to observer is not altered by airlight. However, this assumption is not practical in hazy scene since the light energy radiating from scene points is heavily scattered by atmosphere. Therefore, these applications will fail in bad weather conditions. In consumer photography, the images will be annoying with the presence of fog which decreases the contrast significantly. In aerial photography and satellite remote sensing, the photos are much more easily affected by aerosols. Even in clear days, the rays reflected by the ground will be scattered heavily when they pass through the earths atmosphere, which will make image degraded.

Specifically, to restore the visibility of hazy images is in fact restoring the contrast. However, traditional contrast enhancement techniques, such as histogram equalization, histogram specification and the newly proposed one by Oakley [1], can not be applied to hazy images since the contrast lost in these images is depth-relevant. Recently, many dehazing algorithms based on maximizing the contrast of hazy images have been proposed [2, 3, 4]. All of these algorithms are proven to be simple but effective.

Since there is a lack of ground truth under same lighting condition, the quantitative evaluation of different dehazing algorithms is difficult. According to Tarel's work [5], there are 4 different types of fog, i.e. uniform fog, heterogeneous extinction coefficient fog, heterogeneous luminance fog, heterogeneous both extinction coefficient and luminance fog. Most of current available single image dehazing algorithms assume the fog is uniform and few of them have done quantitative evaluations on scenes with different types of fog.

In this paper we present a general method to recover a haze-free image taking only one photograph as input, which is applicable to all 4 types of hazy images. By assuming the haze-free image have more contrast than image plagued by fog, we restore visibility through maximizing the effect of atmospheric veil, which is equivalent to maximizing the contrast of the resulting image. Based on the observation that the atmospheric veil changes dramatically only alone edges, we adapt the total variation (TV-ℓ_1) [6] minimization framework to preserve discontinuities. Our algorithm is physically plausible and can be used to handle most of the hazy images, including the ones with homogeneous haze and heterogeneous haze . We compare our algorithm with the existing ones, using both true scenes and synthetic ones in [7]. The quantitative evaluation shows the effectiveness of our algorithm.

The remaining of this paper is organized as follows. In Sect. 2, we review the current available algorithms for restoring visibility from hazy images. In Sect. 3, we describes the details of our algorithm. We show our results and perform a quantitative evaluation of our algorithm in Sect. 4. Finally, we conclude this paper and discuss our future work in Sect. 5.

2. RELATED WORK

From an application point of view, dehazing algorithms are very useful in many fields. In remote sensing systems, the quality of sensing is heavily dependent on the weather. In [8], Zhang et al. removes the haze effect in sensing by assuming a uniform haze layer across the image. Haze effect also affects the safety of driving a vehicle. For the camera-based Advanced Driver Assistance System (ADAS), Tarel et al. [9] proposes an automatic fog detection and restoration algorithm in which the onboard camera parameters are leveraged. Regarding the large part of a road image is planar, visibility enhancement dedicated to planar surface was first proposed in [10]. In [5], another algorithm based on the planar assumption is introduced.

Dehazing from a single image is an challenge problem. Early approaches to restore visibility of hazy images focused on achieving the image decomposition with additional information. In [11], the polarized haze effect are removed given two photographs taken under different polarization state. In [12], user interactions is involved to dehaze. Recently, Schaul et al. proposes an algorithm [13] to restore the visibility based on near-infrared (NIR) information and it achieves good results. Kopf et al. [14] utilizes the 3D model of a city to restore the image. For this kind of algorithms, due to more information is utilized, the results is generally impressive.

In the context of computational photography, there is a great progress in single image dehazing [15, 2, 16, 17]. Relying on one or two reasonable assumption(s), the input for the algorithm is a single image. Fattal [15] assumed that the transmission and the surface shading are locally uncorrelated. He first inferred the transmission in the area affected by thin fog and then propagate the transmission to dense fog area. This approach is physically based and achieves good result. However, it fails when all pixels on the image are affected by dense fog. Tan [2] restores the visibility by locally maximizing contrast of the results. Since the contrast is maximize, the results seems to be too saturated. He [18] proposed Dark Channel Prior to solve the single image dehazing problem. It extracts a coarse level transmission map and then refines it using *soft matting*. In He's latter work [19], he substitute the soft matting with *guided filter* which is more computational efficient. Tarel [4] proposed a more fast dehazing algorithm, of which the complexity is linear to the size of input image. *Sparse prior* is also used for dehazing [20].

Most of the dehazing algorithms assume the haze in the scene is homogeneous. The work on removing heterogeneous haze is relatively small. In [7] Tarel first proposes an algorithm working for both homogeneous and heterogeneous haze.

Among all these dehazing algorithms, it is difficult to tell which one is better than the other since there is a lack of ground truth data. In practice, to obtain a pair of images with and without fog is a hard work since it requires to check that the illumination conditions are the same into the scene with and without fog. To our best knowledge, there are mainly two quantatative measurements for the restore image. One is described in [21], the *mean visitable edge ratio* can reflects the quality of the restored image to some extent. The other one is averaged *absolute difference* which is used in [5]. Tarel et al. [5] have already built some synthetic scenes with ground truth for evaluation purpose.

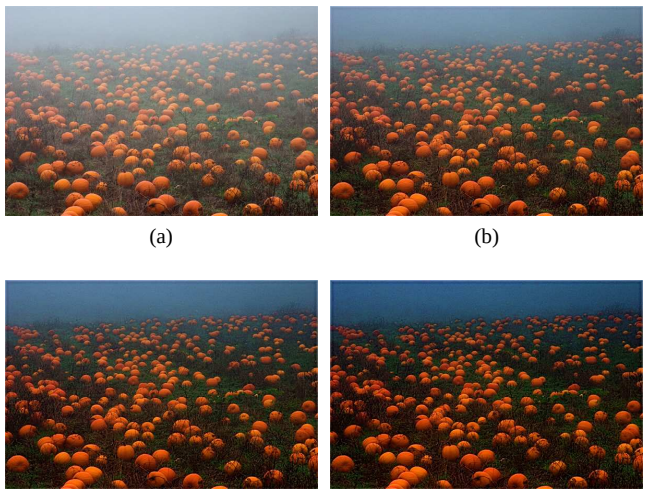

Fig. 1. The effect of β in Eq. (5). (a) The input hazy image. (b)-(d) The dehazing results obtained by setting $\beta = 0.6$, $\beta = 0.8$, $\beta = 0.95$ respectively.

3. OUR ALGORITHM

The model widely used [15, 4, 18, 20] in computer graphics and computer vision to describe the formation of the hazy image is given by the Koschmieder's law:

$$\mathbf{I}(\mathbf{x}) = \mathbf{J}(\mathbf{x})e^{-kd(\mathbf{x})} + \left(1 - e^{-kd(\mathbf{x})}\right)\mathbf{L}_{\infty}, \qquad (1)$$

where $\mathbf{I}(\mathbf{x})$ is the observed hazy image, $\mathbf{J}(\mathbf{x})$ is the haze-free image, k is the extinction coefficient of the haze and $d(\mathbf{x})$ denotes the distance of the object at pixel $\mathbf{x} = (x, y)$. For homogeneous haze, both $\mathbf{L}_{\infty}$ and k are global constants over the whole image; for heterogeneous haze, $\mathbf{L}_{\infty}$ and k may vary locally.

The addend and the augend in Eq. (1) describe two mechanisms of the fog: *direct attenuation* and airlight. Schechner's work [11] describes the two mechanisms in detail.

3.1. Initialization of atmospheric veil

With the concept *atmospheric veil* (or airlight map) $\mathbf{V}(\mathbf{x}) = \mathbf{L}_{\infty}(1 - e^{-kd(\mathbf{x})})$ introduced by Tarel's work [4], Eq. (1) can

be rewritten as,

$$\mathbf{I}(\mathbf{x}) = \mathbf{J}(\mathbf{x})\left(1 - \frac{\mathbf{V}(\mathbf{x})}{\mathbf{L}_\infty}\right) + \mathbf{V}(\mathbf{x}). \tag{2}$$

As suggested by [4], white balance is performed on the hazy image before the visibility restoration algorithm. Once the white balance is correctly performed, the color of the sky $\mathbf{L}_\infty$ can be set to pure white, i.e. $[1,1,1]$. Thus, the atmospheric veil will be the product of $[1,1,1]$ and a scalar map $V(\mathbf{x}) = 1 - e^{-kd(\mathbf{x})}$. For convenience, we call both $\mathbf{V}(\mathbf{x})$ and $V(\mathbf{x})$ the atmospheric veil.

It is easy to see $V(\mathbf{x}) \geq 0$ due to its physical property. To get the maximum value of $V(\mathbf{x})$, we take the minimal of each component in Eq. (2) and it can be rearranged as,

$$\min_{c\in\{r,g,b\}}(\mathbf{I}^c(\mathbf{x})) - \min_{c\in\{r,g,b\}}(\mathbf{J}^c(\mathbf{x})(1 - V(\mathbf{x}))) = V(\mathbf{x}). \tag{3}$$

Since $\min_{c\in\{r,g,b\}}(\mathbf{J}^c(\mathbf{x})) \geq 0$ and $1 - V(\mathbf{x}) \geq 0$, then we get

$$0 \leq V(\mathbf{x}) \leq \min_{c\in\{r,g,b\}}(\mathbf{I}^c(\mathbf{x})). \tag{4}$$

So we can initialize the atmospheric veil as,

$$V_0(\mathbf{x}) = \beta \min_{c\in\{r,g,b\}}(\mathbf{I}^c(\mathbf{x})), \tag{5}$$

where $0 < \beta < 1$ is a constant that relates with the density of the fog. For an image with dense fog, β should be large and otherwise small. On the other hand, β can also be regarded as a parameter controls the strength of the visibility restoration. See Fig. 1 for an example. Equation (5) is applicable for color images and we obviously have $V(\mathbf{x}) = \beta I(\mathbf{x})$ for a gray scale hazy image.

3.2. Atmospheric veil refinement

As described in [4], maximizing the contrast of resulting image is equivalent to maximizing $V(\mathbf{x})$ assuming than $V(\mathbf{x})$ is smooth most of the time,

$$\arg\max_V \int_\Omega V(\mathbf{x}) - \alpha\phi(||\nabla V||^2)dx, \tag{6}$$

where parameter α controls the smoothness of the solution, ϕ is an increasing concave function, $\nabla V(\mathbf{x})$ is the derivatives of the atmospheric veil. Although Eq. (6) allows large jumps in $V(\mathbf{x})$ (since ϕ is concave), unfortunately, it is a non-convex optimization problem and thus the optimal solution may be hard to obtained.

Here, rather than maximizing a non-convex functional, we adapt *total variation minimization*, which was first proposed in image processing by Rudin, Osher and Fatemi (ROF model) [6], to pursing the maximum of the atmospheric veil while allowing discontinuities alone edges.

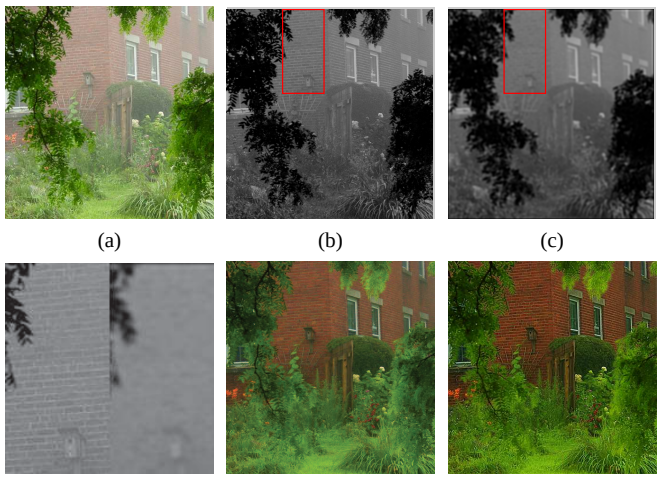

Fig. 2. Single image dehazing with TV-ℓ_1 minimization. (a) The input image. (b) The initialization of atmospheric veil $V_0(\mathbf{x})$. (c) The final atmospheric veil $V(\mathbf{x})$. (d) Zoom in comparision. (e) Result using $V_0(\mathbf{x})$. (f) Result using $V(\mathbf{x})$.

Formally, in our case, we minimize the following energy function to obtain the refined $V(\mathbf{x})$,

$$\arg\min_V \int_\Omega ||V_0 - V||_2^2 + \alpha||\nabla V(\mathbf{x})||_1 dx, \tag{7}$$

where $||\cdot||_n$ denotes ℓ_n norm. $||\nabla V(\mathbf{x})||_1$ in Eq. (7) is called total variation (TV) of $V(\mathbf{x})$.

Our model is physically plausible. In fact, we are pursing such a $V(\mathbf{x})$ that is close to $V_0(\mathbf{x})$ and can only change dramatically along the edges. As illustrated in [22], ℓ_1 norm (total variation) can preserve the discontinuities in the original image well.

To minimize Eq. (7), Euler-Lagrange function can not be applied since the ℓ_1 norm is not differentiable. Here, we adapt the algorithm described by Chambolle [23] to get the solution. To illustrate the algorithm clearly, we give the discrete version of Eq. (7),

$$\arg\min_{\mathbb{V}} ||\mathbb{V}_0 - \mathbb{V}||^2 + \alpha(||\mathbb{D}_x \cdot \mathbb{V}||_1 + ||\mathbb{D}_y \cdot \mathbb{V}||_1), \tag{8}$$

where $\mathbb{V}$ and $\mathbb{V}_0$ are the vectorized version of $V(\mathbf{x})$ and $V_0(\mathbf{x})$ respectively, $\mathbb{D}_x$ and $\mathbb{D}_y$ denote the x- and y- derivative filters, i.e. $\mathbb{D}_x \cdot \mathbb{V} = V * [-1,0,1]$. Then the solution to Eq. (7) given by [23] is the following iterative process,

$$\begin{aligned}
\mathbb{V}^{(i)} &= \mathbb{V}_0 + \alpha(\mathbb{M}^{(i)} + \mathbb{N}^{(i)}),\\
\mathbb{M}^{(i+1)} &= \frac{\mathbb{M}^{(i)} + (\tau/\alpha)\mathbb{D}_x\mathbb{V}^{(i)}}{\max\{1, |\mathbb{M}^{(i)} + (\tau/\alpha)\mathbb{D}_x\mathbb{V}^{(i)}|\}},\\
\mathbb{N}^{(i+1)} &= \frac{\mathbb{N}^{(i)} + (\tau/\alpha)\mathbb{D}_y\mathbb{V}^{(i)}}{\max\{1, |\mathbb{N}^{(i)} + (\tau/\alpha)\mathbb{D}_y\mathbb{V}^{(i)}|\}},
\end{aligned} \tag{9}$$

where $\tau > 0$ called "time-step" in [23] and should be $\tau \leq 1/4$ to make the iteration converged, $|\cdot|$ is the absolute value op-

(a) Tarel (b) Our algorithm

Fig. 3. Comparison with Tarel's methods. The input image is shown in Fig. 2(f). (a) The result obtained by [4]. (b) The result obtained by our algorithm. Note that in the red rectangle region, due to the sharp variations in depth, [4] can not process it well.

erator and is performed element-wise on a vector. As suggest by [23], we set $0.24 \leq \tau \leq 0.249$ during our experiment and a good convergence can be obtained.

3.3. Visibility restoration

Once the atmospheric veil $V(\mathbf{x})$ is estimated, each color component of the haze-free image $\mathbf{J}(\mathbf{x})$ can be restored through Eq. (1). However, as illustrated in [18], the directly recovered intensity is prone to noise when $V(\mathbf{x})$ is too close to 1. Therefor, we restrict the atmospheric veil $V(\mathbf{x})$ to a upper bound V_b, which means a small certain amount of haze are preserved in very dense haze regions. The final intensity is recovered by,

$$\mathbf{J}(\mathbf{x}) = \frac{\mathbf{I}(\mathbf{x}) - \min(V(\mathbf{x}), V_b)}{1 - \min(V(\mathbf{x}), V_b)} \tag{10}$$

In our experiments, we set $V_b = 0.9$ for all results.

4. RESULTS AND EVALUATIONS

In our experiments, we implement our algorithm using C++. It takes about 1-2 seconds to get the final dehazing results for a 600×480 hazy image on a PC with Intel Core^{TM} i7-2600 processor and 8GB installed RAM. As illustrated in [22], the process described by Eq. (9) converges after about 40-50 iterations. So we set a fixed iteration number $n = 70$ for our results.

We have done several experiments, including true scenes and synthetic scenes, to demonstrate our method can generate good results.

Figure 3 shows the comparison with Tarel's [4] work. Note the region marked with red rectangle. Due to the sharply varied depth in this region, [4] can not process it well while our algorithm can.

Figure 4 shows the results of our method compared with 4 start-of-the-art algorithms on dehazing. Among the 4 algorithms, Kopf et al. [14] utilize the 3D model of the city to remove haze. Although the input for our algorithm is a single image, our result is visually similar to Kopf's.

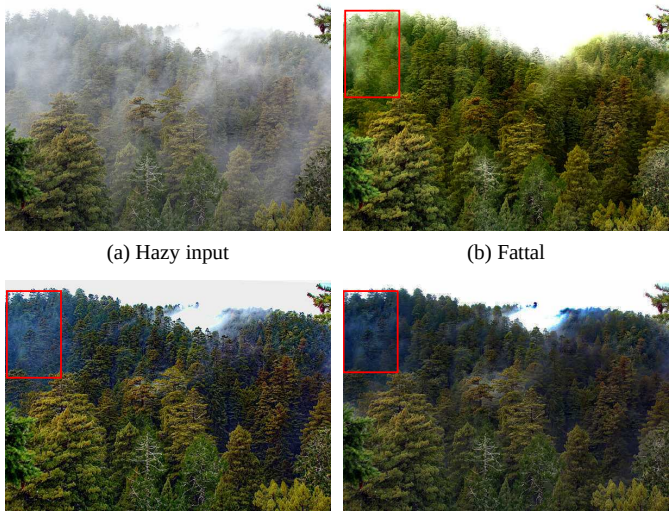

(a) Hazy input (b) Fattal

(c) Tarel (d) Our method

Fig. 5. The results of applying our algorithm on heterogenous fog. (a) The original hazy image. (b)-(d) The results obtained by Fattal [15], Tarel et al. [4] and our algorithm. Our results looks more natural than the other two.

Table 1. The averaged *absolute difference* between restored image of 5 evaluated algorithms and the groundtruth.

Algorithm	Uniform	Variable k	Vari. $\mathbf{L}_\infty$	Vari. k&$\mathbf{L}_\infty$
Fattal	36.7 ± 4.2	$\mathbf{38.2 \pm 3.0}$	42.8 ± 6.2	44.7 ± 5.9
Tan	45.2 ± 4.0	44.0 ± 3.4	42.9 ± 12.8	49.1 ± 4.4
He et al.	33.2 ± 2.3	42.0 ± 9.2	41.0 ± 6.9	42.3 ± 8.6
Tarel et al.	46.7 ± 3.4	41.2 ± 7.1	47.3 ± 4.2	39.5 ± 5.8
Ours	$\mathbf{31.5 \pm 4.5}$	40.5 ± 4.0	$\mathbf{39.8 \pm 7.9}$	$\mathbf{37.2 \pm 7.3}$

Although our algorithm is designed for homogeneous fog, we can also apply it to the scenes with heterogenous fog. Figure 5 shows an example scenes. We also compare our result with the ones generated by Fattal [15] and Tarel et al. [4]. All three algorithms can not remove the fog totally (see the area with red rectangle), but our result looks more natural than the other two.

To quantitatively evaluate our algorithm, we calculate the averaged absolute difference between the restored image and the true haze-free image of the same scene. We utilize the synthetic image pairs built by Tarel et al. [5] using SiVIC^{TM} for evaluation. Here, we quantitatively evaluate 4 other algorithms that proposed by Fattal [15], by Tan [2], by He [18] and by Tarel [4].

Following [5, 7], we calculate the averaged absolute difference between the image without fog and the restored image to measure the similarity between them. The result is shown in Tbl. 1. The mean and the stand deviation is calculated over all images.

(a) Hazy input (b) Tan (c) Fattal (d) He (e) Kopf (f) Our algorithm

Fig. 4. Comparison with 4 stat-of-the-art dehazing algorithms. (a) The original hazy image. (b)-(e) The results obtained by Tan [2], Fattal [15], He [18] and Kopf [14] respectively. (f) The result obtained by our algorithm.

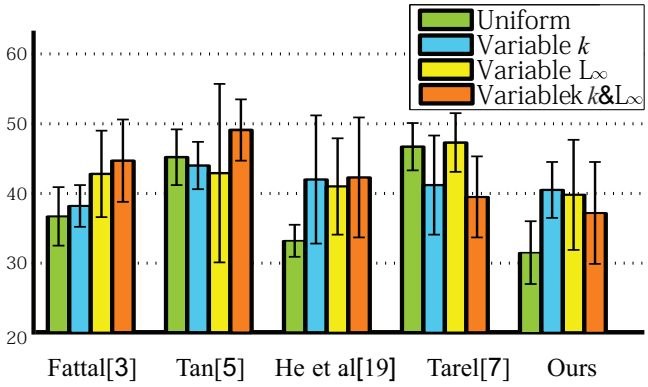

Fig. 6. The illustration of the results of quantitative evaluation of 5 evaluated algorithms.

Figure 6 shows the averaged absolute difference and the variance of different methods. From Tbl. 1 and Fig. 6, we conclude that our algorithm outperforms most state-of-the-art dehazing algorithms in case the fog is uniform. For heterogeneous k fog, a more suitable algorithm is Fattal's [15] algorithm. The reason lies in it estimates the atmospheric color locally. Our algorithm is comparable with it. As to heterogeneous $\mathbf{L}_\infty$ fog and heterogeneous k and $\mathbf{L}_\infty$ fog, our algorithm and [4] is more effective.

Figure 7 shows some sample results of our algorithm on the synthetic scenes generated by [5]. We select the scenes with homogeneous and heterogeneous haze to demonstrate our algorithm can process various types of hazy scenes. Refer to the caption of Fig. 7 for more details.

5. CONCLUSIONS AND FUTURE WORK

In this paper, we have proposed a new algorithm to remove haze from a single image using TV-ℓ_1 minimization method. TV-ℓ_1 can preserve the large jumps in atmospheric veil map and easy to implement. Moreover, it is a physically plausible method. Results shows this algorithm can deal with most of the hazy images. The evaluations demonstrate our algorithm outperforms many state-of-the-art dehazing algorithms.

For future work, we intend to concentrate on the current constraints of our method. As shown in Fig. 7, this algorithm performs poor when there is large-scale atmosphere-color-like object in the hazy images. To deal with this regions, we plan to segment them out first and treat them specially.

6. REFERENCES

[1] J. Oakley and H. Bu, "Correction of simple contrast loss in color images," *IEEE Trans. on Image Process*, vol. 16, no. 2, pp. 511–522, 2007.

[2] R. Tan, "Visibility in bad weather from a single image," in *CVPR*, 2008.

[3] J.-H. Kim, J.-Y. Sim, and C.-S. Kim, "Single image dehazing based on contrast enhancement," in *ICASSP*, 2011.

[4] J.-P. Tarel and N. Hautière, "Fast visibility restoration from a single color or gray level image," in *ICCV*, 2009.

[5] N. Hautière, J.-P. Tarel, and D. Aubert, "Mitigation of visibility loss for advanced camera based driver assistances," *Trans. on Intelligent Transportation Systems*, vol. 11, no. 2, pp. 474–484, 2010.

[6] L. Rudin, S. Osher, and E. Fatemi, "Nonlinear total variation based noise removal algorithms," *Physica. D*, vol. 60, pp. 259–268, 1992.

[7] J.-P. Tarel, N. Hautière, A. Cord, D. Gruyer, and H. Halmaoui, "Improved visibility of road scene images under heterogeneous fog," in *IEEE Intelligent Vehicles Symposium*, 2010.

[8] Y. Zhang, B. Guindon, and J. Cihlar, "An image transform to characterize and compensate for spatial variations in thin cloud contamination of landsat images," *Remote Sensing of Environment*, vol. 82, no. 2, pp. 173–187, 2002.

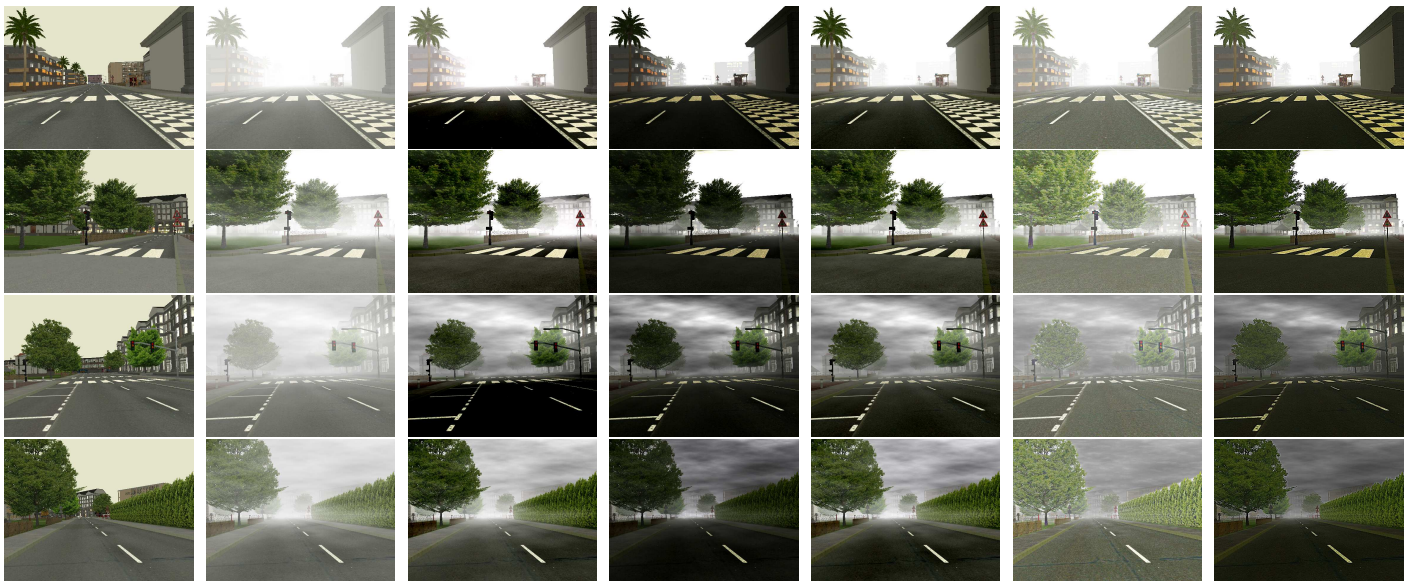

(a) GT (b) With fog (c) Fattal (d) Tan (e) He et al. (f) Tarel et al. (g) Our algorithm

Fig. 7. Sample results of quantitative evaluation of our algorithm on the synthetic scenes generated by [5]. (a) The image without fog. (b) The hazy image. (c)-(e) The results obtained by Fattal [15], Tan [2], He et al. [18], Tarel et al.[4] and our algorithm. 1st row: scene sample with uniform fog. 2nd row: scene sample with heterogeneous k fog. 3rd row: scene sample with heterogeneous $\mathbf{L}_\infty$ fog. 4th row: scene sample with heterogeneous k and $\mathbf{L}_\infty$ fog.

[9] N. Hautière, J.-P. Tarel, J. Lavenant, and D. Aubert, "Automatic fog detection and estimation of visibility distance through use of an onboard camera," *Machine Vision and Applications*, vol. 17, no. 1, pp. 8–20, 2006.

[10] N. Hautière and D. Aubert, "Contrast restoration of foggy images through use of an onboard camera," in *IEEE Trans. on Intelligent Transportation Systems*, 2005, pp. 601–606.

[11] Y. Schechner, S. Narasimhan, and S. Nayar, "Instant dehazing of images using polarization," in *CVPR*, 2001.

[12] S. Narasimhan and S. Nayar, "Interactive deweathering of an image using physical models," in *IEEE Workshop on Color and Photometric Methods in Computer Vision*, 2003.

[13] L. Schaul, C. Fredembach, and S. Süsstrunk, "Color image dehazing using the near-infrared," in *ICIP*, 2009.

[14] J. Kopf, B. Neubert, B. Chen, M. Cohen, D. Cohen-Or, O. Deussen, M. Uyttendaele, and D. Lischinski, "Deep photo: Model-based photograph enhancement and viewing," *ACM Trans. on Graphics*, vol. 27, no. 5, 2008.

[15] R. Fattal, "Single image dehazing," *ACM Transaction on Graphics*, vol. 27, no. 3, pp. 1–9, 2008.

[16] J. Zhang, L. Li, G. Yang, and Y. Zhang, "Local albedo-insensitive single image dehazing," *The Visual Computer*, vol. 26, no. 6-8, pp. 761–768, 2010.

[17] E. Matlin and P. Milanfar, "Removal of haze and noise from a single image," in *SPIE Conference on Computational Imaging*, 2012.

[18] K. He, J. Sun, and X. Tang, "Single image haze removal using dark channel prior," in *CVPR*, 2009.

[19] K. He, J. Sun, and X. Tang, "Guided image filtering," in *ECCV*, 2010.

[20] L. Kratz and K. Nishino, "Factorizing scene albedo and depth from a single foggy image," in *ICCV*, 2009.

[21] N. Hautière, J.-P. Tarel, D. Aubert, and E. Dumont, "Blind contrast enhancement assessment by gradient ratioing at visible edges," *Image Analysis & Stereology Journal*, vol. 27, no. 2, pp. 87–95, 2008.

[22] A. Chambolle, V. Caselles, M. Novaga, D. Cremers, and T. Pock., "An introduction to total variation for image analysis," `http://hal.archives-ouvertes.fr/docs/00/43/75/81/PDF/preprint.pdf`, 2009.

[23] A. Chambolle, "Total variation minimization and a class of binary mrf models," in *EMMCVPR*, 2005.